Three-dimensional nonlinear electromagnetic field computations, using scalar potentials

J. Simkin, B.Sc., and C.W. Trowbridge, B.Sc., C.Eng., F.I.E.E.

Indexing terms: Electromagnetics, Computer applications, Nonlinear systems

Abstract: A formulation based on scalar potentials for the numerical solution of three-dimensional nonlinear static electromagnetic field problems is presented. The resulting equations are solved using finite elements, based on a Galerkin procedure. A general-purpose package called TOSCA has been developed, implemented and tested. Results are presented for three cases and compared with measured values.

List of principal symbols

$\boldsymbol{B}$ = magnetic flux density
$\boldsymbol{H}$ = magnetic field intensity
$\boldsymbol{J}$ = current density
$\boldsymbol{H}_e$ = coercive field intensity
μ = permeability
ψ = magnetic scalar potential
φ = reduced magnetic scalar potential
$\hat{n}$ = unit outward normal vector
$\hat{t}$ = unit surface tangent vector

1 Introduction

Electromagnetic fields are important in industrial and scientific applications. The scale of production of particular devices varies tremendously, but in all cases, computer solutions for the fields play an essential part in their design. Very accurate results can be obtained if the fields are essentially two-dimensional, [1] but the same is not true when the fields are three-dimensional.

Three-dimensional solutions have been obtained by solving either integral[2] or differential equations.[3] The integral operator formulation has many advantages for magnetostatic computations: only the iron and coils are specified, there is no mesh in the air; in addition, the solution is naturally bounded at infinity rather than at the mesh boundary, as would be true of a differential operator method. However, there are also disadvantages: complicated geometry causes a tremendous escalation in the cost; recovering flux densities from the solution is expensive; flux densities close to the surface of magnetic materials are strongly affected by the discretisation.

In general, the solution of integral equations has given the best results when the problem geometry was simple. For the linear case, i.e. a problem for which the material permeability is independent of field, the domain of the integral equation reduces from volumes to surfaces, thus simplifying the mesh and decreasing the cost considerably. Some of the disadvantages of the integral approach can be avoided by solving the corresponding partial differential equation; however, algorithms based on differential operators have none of the advantages mentioned above. For these reasons, both approaches, separately and in combination, will continue to excite interest and be used in the computer solution of field problems; however, the method presented in this paper is based on the differential operator.

Partial differential equations can be solved by discretising the domain of the operator into finite elements. However, it is not obvious which formulation of the three dimensional magnetostatic problem will lead to an efficient computer algorithm. For the calculation of two-dimensional fields, the magnetic vector potential has been widely used [4, 5]. The extension of this approach to three-dimensional fields leads to unnecessary complications. The potential has three components, and its gauge must be specified, either by using penalty functions or putting the gauge information into the operator - which provides a difficult interface boundary condition. It is only the electric currents that make it necessary to use a potential that can specify a rotational field.

A scalar potential can be used, provided that special provision is made for the fields from electric currents. The methods proposed [6,7] have involved expressing the total field as the sum of two parts; the first from electric currents being obtained by direct integration from the known currents; the second resulting from the interaction of the current fields with magnetic materials, and this can be represented as the gradient of a scalar potential (the reduced potential). It has been shown8 that this approach gives rise to a severe loss of precision caused by cancellation between the separately-computed parts of the total field. The solution to this problem8 is the coupling together of differently-defined scalar potentials; where necessary (e.g. inside conductors), the reduced scalar potential is used, and elsewhere a scalar potential whose gradient is the total field. This has been shown to be effective in two dimensions.[8] In this paper, the method is extended to three dimensions and its efficiency is demonstrated by comparison of measurements with computed results obtained by the TOSCA code. The code is based on the total scalar potential formulation presented in this paper and can be used for a wide class of static problems

The use of a total field scalar potential is also of interest for integral equation formulations.[9] It gives a more stable and accurate solution than that obtained by other approaches. However, for nonlinear problems, the disadvantages of integral methods still apply.

Paper 912B, first received 24th April and in revised form 17th July 1980
The authors are with the Computing Applications Group, Technology Division, Rutherford and Appleton Laboratories, Chilton, Didcot, Oxfordshire OX 11 OQX, England

0143-7038/80/060368 + 07 $01.50/0

2 Formulation of the defining equations

2. 1 Basic equations of nonlinear magnetostatics [IO]

The following subset of Maxwell's equation describes the nonlinear magnetostatic field

$$\text{Div}\, \boldsymbol{B} = 0 \tag{1}$$

$$\text{Curl}\, \boldsymbol{H} = \boldsymbol{J} \tag{2}$$

where $\boldsymbol{B}$ is the magnetic induction, H the field intensity and $\boldsymbol{J}$ the current density, which is a known function. The magnetic induction and the field intensity are related by a constitutive equation of the form

$$\boldsymbol{B} = \mu(\boldsymbol{H})(\boldsymbol{H} - \boldsymbol{H}_c) \tag{3}$$

where μ is the material permeability.

For nonlinear problems, μ is a function of $\boldsymbol{H}$ and, in general, it may be a tensor. $\boldsymbol{H}_c$ is the material's coercive field. In 'soft' magnetic materials, the coercive field intensity is normally assumed to be zero; 'hard' magnetic materials, e.g. permanent magnets, have nonzero coercive field intensity.

2.2 Derivation of the magnetic scalar potential

If, in a region of space Ω

$$\text{Curl}\, \boldsymbol{H} = 0$$

then $\boldsymbol{H}$ can be represented as the gradient of a scalar potential

$$\boldsymbol{H} = -\nabla \psi \tag{4}$$

The scalar potential ψ whose gradient gives the total field will be called the total scalar potential.

If, in a region of space Ω_j

$$\text{Curl}\, \boldsymbol{H} \neq 0$$

i.e. Ω_j contains electric currents, but not necessarily everywhere, the $\boldsymbol{H}$ can be separated into two parts

$$\boldsymbol{H} = \boldsymbol{H}_m + \boldsymbol{H}_s \tag{5}$$

where $\boldsymbol{H}_s$ is the field produced by all the currents contained in Ω_j and H_m is the rest of the field. With this partitioning of the field

$$\text{Curl}\, \boldsymbol{H}_m = 0$$

and $\boldsymbol{H}_m$ can be represented as the gradient of a scalar potential (the reduced scalar potential)

$$\boldsymbol{H}_m = -\nabla \phi$$

The field $\boldsymbol{H}_s$ can be found for any prescribed currents by evaluation

$$\boldsymbol{H}_s = \frac{1}{4\pi} \int_{\Omega_j} \boldsymbol{J} \times \nabla \left(\frac{1}{R} \right) d\Omega \tag{6}$$

where $\boldsymbol{J}$ is the current density and $\boldsymbol{R} = |\boldsymbol{r} - \boldsymbol{r}'|$ is the distance from the source point $\boldsymbol{r}'$ and the field point $\boldsymbol{r}$ [11].
In some cases, this can be integrated to give a closed form expression for $\boldsymbol{H}_s$; for complicated current paths, the expression can be evaluated by a combination of analytic integration and numerical quadrature.

2.3 The reduced scalar potential approach

Separating the magnetostatic field into two parts, as shown in eqn. 5, immediately gives an attractive formulation, and this has been used to obtain solutions by solving

$$-\nabla \mu \nabla \phi + \nabla \mu \boldsymbol{H}_s = 0 \tag{7}$$

for the unknown ϕ, by the finite-element method[7]. Here $\mathbf{H}_s$ is computed directly from eqn. 6.

However, in magnetic materials, the two parts of the field $\boldsymbol{H}_m$ and $\boldsymbol{H}_s$ tend to be of similar magnitude but opposite direction. Therefore cancellation occurs in computing the field intensity $\boldsymbol{H}$, which gives a loss in accuracy.[8] The effect of this is that the results can become very inaccurate when μ is large. It is clear that the total scalar potential should be used to avoid the cancellation, but this cannot be used to solve the whole problem, since it cannot fully describe the fields produced by electric currents.

2.4 The two-potential approach

Both total scalar potentials and reduced scalar potentials must be combined to avoid the cancellation associated with reduced potentials and yet allow the inclusion of electric currents[8]. In regions Ω_j that contain currents, the reduced scalar potential must be used, and elsewhere the total scalar potential. The solutions must be coupled at the interfaces of the regions. Consider a two-region problem as shown in Fig. 1; in region Ω_j there are currents and the permeability is constant; in region Ω_k there are volumes of magnetic material and no currents.

In Ω_k

$$-\nabla \mu \nabla \phi + \nabla \mu \boldsymbol{H}_s = 0 \tag{8}$$

In Ω_k

$$-\nabla \mu \nabla \phi - \nabla \mu \boldsymbol{H}_c = 0 \tag{10}$$

At the interface T_{kj} between regions Ω_j and Ω_k the normal component of the magnetic induction (B) and the tangential components of the field intensity (ll) must be continuous. If $\hat{n}$ is the outward normal from Ω_k, and $\hat{t}$ a tangent direction to T_{kj} then

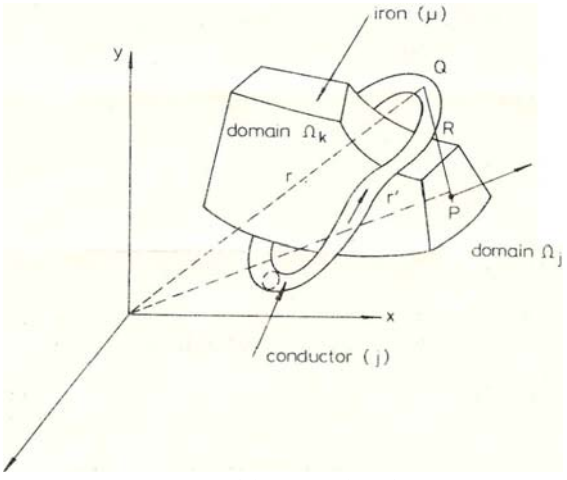

Fig. 1 *Potential domains and topology*

Ω_k: iron ($\nabla \mu \nabla \psi = 0$)
Ω_j : free space ($\nabla^2 \phi = 0$)

$$B_k \hat{n}_k = B_j \hat{n}_k$$

or

$$\mu_k\left(-\nabla\psi - H_c\right)\hat{n}_k = \mu_j\left(-\nabla\phi + H_s\right)\hat{n}_k \tag{10}$$

and

$$H_k\hat{t} = (H_s + H_m)\hat{t}$$

or

$$-\nabla\psi\hat{t} = \left(-\nabla\phi + H_s\right)\hat{t} \tag{11}$$

Equation 11 can be integrated over any path on T_{Jk} to give an integral relationship between the potentials at two points *(A* and *B)*

$$\psi_A - \psi_B = \phi_A - \phi_B + \int_A^B H_s\hat{t}ds \tag{12}$$

where $\boldsymbol{H}_s$ is obtained explicitly from eqn. 6.

2.5 Other approaches

There are several alternative approaches to the formulation of three-dimensional electromagnetic fields using scalar potentials. In both of the above methods, the fields from prescribed currents are taken out of the partial differential equation, and included directly by evaluating eqn. 6.

This has advantages for solutions obtained using finite elements, since the conductors become independent of the mesh. However, it is possible to devise methods that require the conductors to be included in the mesh, thus avoiding evaluating eqn. 6. The ***T-Ω*** method[18] is perhaps the most well known of these. In this method, ***T*** *is* found by solving a partial differential equation, whose limits are the conductor volumes. ***T*** and $\boldsymbol{H}_s$ only differ by the gradient of scalar potential, but they are evaluated in very different ways.

3 Finite-element method

3.1 Weighted residuals

For a complete derivation of weighted residual methods and the Galerkin method in particular, see Reference 12. The problem is as follows: it is required to solve a partial differential equation of the general form

$$\nabla\alpha\nabla u(r) = Q(r) \quad : r \in \Omega$$

subject to

$$\alpha\frac{\partial u}{\partial n}(r) - p(r) = 0 \quad : r \in \mathrm{T}_1 \tag{13}$$

and

$$u(r) - u_0 = 0 \quad : r \in \mathrm{T}_2$$

where the surfaces T_1 and T_2 form the boundary of n, and u is to be approximated by a set of basis functions

$$u = \hat{u} = \sum N_i u_i \tag{14}$$

The u_i are a set of parameters that determine the approximate solution and the N_j are a set of prescribed functions. In the finite element method, the space Ω is discretised into elements, the N_i are simple polynomials spanning the elements and the u_i are nodal parameters.

A solution to the problem can be obtained by constructing a set of weighted residuals:

$$R_i = \int_\Omega W_i\left(\nabla\alpha\nabla\hat{u} - Q\right)d\Omega + \int_{\mathrm{T}_1}\bar{W}_i\left(\alpha\frac{\partial\hat{u}}{\partial n} - p\right)d\mathrm{T} + \int_{\mathrm{T}_2}\bar{\bar{W}}_i\left(u - u_0\right)d\mathrm{T} = 0 \tag{15}$$

where the $W_i, \bar{W}_i$, and $\bar{\bar{W}}_i$ are an arbitrary set of weighting functions. It is convenient to use integration by parts to reduce the order of continuity required for the functions $\hat{u}$. In this case, integration by parts of the first term in the above equation gives

$$\int_\Omega W_i\left(\nabla\alpha\nabla\hat{u} - Q\right)d\Omega = -\int_\Omega\nabla W_i\alpha\nabla\hat{u}d\Omega + \int_\mathrm{T} W_i\alpha\frac{\partial\hat{u}}{\partial n}d\mathrm{T} - \int_\mathrm{T} WQ_i d\mathrm{T} = 0 \tag{16}$$

and choosing $\bar{W}_i = -W_i$ eliminates the normal gradient term along the boundary T_1. Thus eqn. 15 becomes

$$R_i = -\int_\Omega\nabla W_i\nabla\alpha\nabla\hat{u}d\Omega - \int_\Omega W_i Q d\Omega + \int_{\mathrm{T}_1}\bar{W}_i p d\mathrm{T} + \int_{\mathrm{T}_1} W_i\left(\alpha\frac{\partial\hat{u}}{\partial n}\right)d\mathrm{T} + \int_{\mathrm{T}_2}\bar{\bar{W}}_i\left(u - u_0\right)d\mathrm{T} = 0 \tag{17}$$

The Galerkin method requires the *Wj* to be identified with the basis functions.

That is

$$W_i = N_i \tag{18}$$

As a consequence of this, since the N_i are functions local to elements containing the nodal parameter u_i, eqn. 17 defines a set of algebraic equations based on the weighting functions *(N_i)* and hence on the nodes. The boundary condition on T_2 is usually enforced and therefore the appropriate residuals are eliminated.

The problem has been reduced to the solution of a set of linear equations of the form

$$Au_i = C \tag{19}$$

with

$$A_{ij} = \int_\Omega\nabla N_i\alpha\nabla_j d\Omega \tag{20}$$

The matrix ***A*** is sparse, symmetric and positive definite for this particular choice of weighting functions.

$$C_i = \int_\Omega N_i Q d\Omega \tag{21}$$

3.2 The two-scalar potential (ψφ) formulation

Here the problem is divided into two regions, Ω_k and Ω_j (Fig. 1). In each region, a finite element subdivision is made; however, the problem is not completely defined,

for on the boundary T_{jk}, interface conditions for the

potential and its normal derivatives are available (eqns. 10 and 11), rather than boundary conditions as described in Section 3.1. This gives a more general result for integration by parts (eqn. 16) which must include another term for the interface T_{jk}.

That is: $\int_T W_i \frac{\partial \hat{u}}{\partial n} d\mathrm{T}$

Applying the Galerkin method to each region independently,

$$R^k{}_i = -\int_{\Omega_k} \nabla W_i \mu \nabla \psi \, d\Omega + \int_{T_{1k}} W_i \left(\mu \frac{\partial \psi}{\partial n} \right) d\mathrm{T} + \int_{T_1 k} W_i p \, d\mathrm{T} - \int_{\Omega_k} W_i \nabla \mu \boldsymbol{H}_c \, d\Omega = 0 \tag{22}$$

and

$$R^j{}_i = -\int_{\Omega_j} \nabla W_i \nabla \phi \psi \, d\Omega + \int_{T_{1k}} W_i \left(\mu \frac{\partial \phi}{\partial n} \right) d\mathrm{T} + \int_{T_1 j} W_i p \, d\mathrm{T} = 0 \tag{23}$$

where μ_j has been removed, since it is assumed constant in the region Ω_j.

Furthermore, requiring $R_i^j + R_i^k = 0$, using the interface conditions (eqns. 10 and 12) and continuity of the weight functions between Ω_j and Ω_k gives (T_{1j} and T_{1k} are the portions of T_j on which normal derivative boundary conditions are imposed):

$$\int_{\Omega_k} \nabla W_i \mu \nabla \psi \, d\Omega + \int_{\Omega_j} \nabla W_i \nabla \phi \, d\Omega = -\int_{T_{jk}} W_i \left(H_s \hat{n} \right) d\mathrm{T} - \int_{\Omega_k} W_i \nabla \mu \boldsymbol{H}_c \, d\Omega + \int_{T_{1j}} W_i p \, d\mathrm{T} + \int_{T_{1k}} W_i p \, d\mathrm{T} \tag{24}$$

After applying the Galerkin method to eqn. 24 with a finite-element discretisation, the coefficient matrix is identical to eqn, 20 with appropriate permeability. At the interface T_{jk}, either φ_i or ψ_i can be eliminated by eqn. 12. Eliminating φ results in a right-hand side term for a node on the interface that is given by

$$C_i = A g_i - h_i \tag{25}$$

where

$$g_i = \int_0^{t_i} \boldsymbol{H}_s \, dt \tag{26}$$

$$h_i = \int_{T_{jk}} N_i \boldsymbol{H}_s \hat{n}_k \, d\mathrm{T} \tag{27}$$

3.3 Numerical methods used in the program

In each region, a finite-element subdivision is made and a standard assembly procedure is followed. The contribution to the matrix $\boldsymbol{A}$ from an element is of the form (c.f. eqn. 20)

$$a_{ij} = \int_{\Omega_e} \mu \left(\frac{\partial N_i}{\partial x} \frac{\partial N_j}{\partial x} + \frac{\partial N_i}{\partial y} \frac{\partial N_j}{\partial y} + \frac{\partial N_i}{\partial z} \frac{\partial N_j}{\partial z} \right) d\Omega \tag{28}$$

where Ω_e is the volume of the element. The contribution to the right-hand sides from an element with a node (l) on the interface T_{jk} is

$$c_i = a_{li} g_l \tag{29}$$

where g is given by eqn. 26.

If the element possesses a facet that forms part of T_{jk}, its contribution to the right-hand side will include

$$c_i = \int_{facet} N_i \boldsymbol{H}_s \hat{n} \, d\mathrm{T} \tag{30}$$

The TOSCA program uses 8-, or 20-node isoparameteric brick elements. The element coefficients are evaluated by Gaussian quadrature. An absolute relationship between φ and ψ must be specified at least at one point on the interface to ensure uniqueness. This was normally done by setting both to zero on a plane of symmetry, but a single point was used if the interface surface did not meet a plane of symmetry. The relationship between φ and ψ at other points on an interface was then found from eqn. 12 by Gaussian quadrature along paths in the interface. This was done incrementally, moving from a node to its neighbour on the interface, in the same facet. A wide range of conductor geometries were available [13].

The resulting system of linear equations were solved using a preconditioned conjugate gradient method[34]. Nonlinear permeabilities were included by updating the permeabilities after each solution and solving again. This process was repeated until convergence was achieved.

3.4 Forces

Many problems require the evaluation of forces obtained by integrating the 'Maxwell stress' $B^2/2\mu_0$ over defined surfaces in free space. If the force on a particular region of iron is required, then the most convenient procedure is to integrate the three force components over each surface element of the region of interest. The condition defining the direction of the force is given by

$$\boldsymbol{n.B = (B.F)/|F|} \tag{31}$$

where the coplanar vectors $\boldsymbol{n}$, $\boldsymbol{B}$ and $\boldsymbol{F}$ are the normal, total field and total force vectors, respectively, at a surface point. The vector $\boldsymbol{B}$ is obtained from the finite element shape functions and the forces are then integrated numerically by Gaussian quadrature in the usual way.

In general, the element size can never be reduced such that variations in the potential of higher order than the element shape function can be neglected. This is important with nonrectangular 8-node isoparametric brick elements if the shape-function derivatives are used to compute field values. The cross terms in the shape functions (e.g. *xy)* give a strong coupling between the element distortion, the higher-order potential variations and the field values.

Higher-order elements avoid this difficulty. Rectangular elements are essential on the surfaces where Maxwell stress integrations are carried out if 8-node brick elements are used.

4 Results

The first release of the *TOSCA* program runs as a 'batch job'; interactive data preparation and result retrieval are not possible, although some data checking via 'batch graphics' has been provided. The finite-element mesh is developed by automatically subdividing hexahedra into elements. If a problem consists of rectangular geometry, the whole process has been made automatic and only the leading dimensions have to be supplied - a regular topology rectangular mesh is produced. More complex geometries can be handled by another mesh generation macro that allows an irregular topology mesh in one plane, regular in the third dimension. As well as solving magnetostatic problems with hard or soft magnetic materials, the code can also be used for electrostatic solutions, including volume charges.

4. 1 Type 1 bending magnet

For this test a magnet showing large nonlinear effects was used. The Rutherford Laboratory type 1 bending magnet shows a 17% departure from linearity of its central field for a current of 450 A*. The magnet is made of two different types of steel, and the geometry is shown in Fig. 2. Fig. 3 shows the variation in field along the axis of the magnet, measured and computed, and Fig. 4 the error in the computed solution as a percentage of the central field.

4.2 Vernier linear motor

This problem was posed by J.W. Finch†. The motor has a small air gap and its fields are strongly influenced by saturation of the iron yoke. The geometry is shown in Fig. 5. An integral equation solution has been used to compute the force on the movable 'rotor' as a function of displacement out of the yoke gap. Poor results were obtained because the fields in the airgap were strongly affected by the problem discretisation. The same problem was solved using the TOSCA program; measured and computed forces as function of displacement are shown in Fig. 6. A refined mesh in the region of the airgap and rotor had to be used to achieve this accuracy. Approximately 8000 nodes were required and the solution time was of the order of 25 min, (IBM *360/195)*

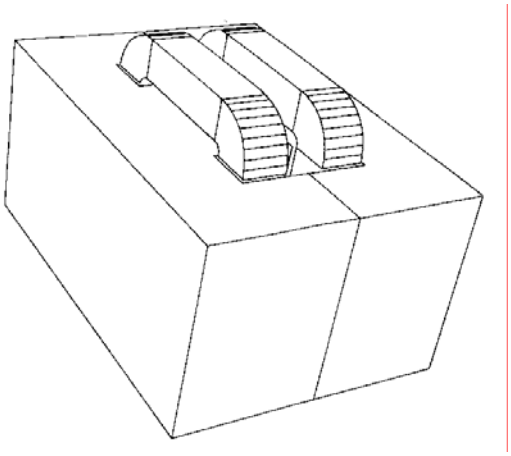

Fig. 2 *Geometry of type I bending magnet*

4.3 Stepping motor

The geometry of the stepping motor is shown in Fig. 7. Inductance calculations on a two-dimensional computer program had shown good agreement with measurement for some rotor positions, but very poor agreement for other positions ‡. Good agreement was obtained when the rotor teeth were aligned with the poles of the stator that carry coils. In this case the airgap is very small. When the rotor

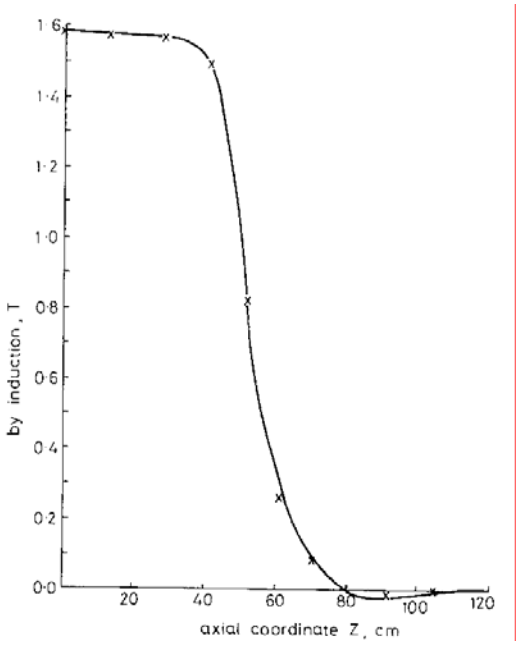

Fig. 3 *Flux density as a function of axial position for type 1 bending magnet (using 5200 8-node brick elements)*
——— measured
X computed

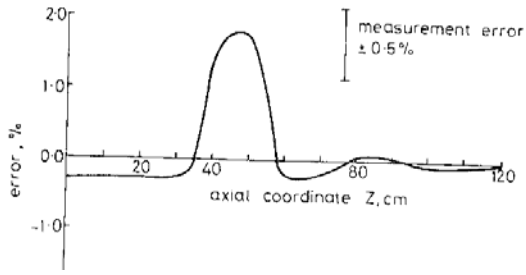

Fig. 4 *Error in computed solution for type 1 bending magnet*

• NEWMAN, M.J.: Private communication. RITCHIE, P.J.S., and LOACH. B.G.: 'Nimrod beam line equipment data handbook' (Rutherford Laboratory. 1968)
† FINCH. J.W.: Department of Electrical Engineering, University of Newcastle, Private communication

* STEPHENSON, M.: Department of Electrical Engineering, University of Leeds. Private communication

slots were aligned with the same poles, values for computed and measured inductances disagreed. In this case the airgap of the motor was large compared to its length and the errors were thought to be caused by this. An analysis of a three-dimensional model of this motor was carried out using the TOSCA program. The results are shown in Table 1; the agreement for the case when the slots are aligned is much better. Each case took 15 nun c.p.u. time.

Table 1: Computed and measured inductances for the stepping motor

A Rotor teeth aligned with stator poles			
Current	Measured	Computed inductance, mH	
Amps	inductance, mH	2Dmodel	3D (TOSCA)
4	111	111	116
8	66	66.5	68
B Rotor slots aligned with stator poles			
Current	Measured	Computed inductance, mH	
Amps	inductance, mH	20 model	3D (TOSCA)
4	19.8	13.2	20.6
8	19.8	13.2	20.5

5 Conclusions

A three-dimensional finite-element program (TOSCA) has been developed in order to examine the effectiveness of the two-scalar potential solution for magnetostatic field problems. The results shown in this paper clearly demonstrate that the method is effective for a wide range of cases. The method appears most efficient for the calculation of forces and inductances, which are areas where integral equation solutions often prove to be intractable. There is a problem when accurate field values or gradients are required; and here, differentiating the finite-element shape functions to obtain fields gives results that display element structure. This is particularly true with low-order elements (e.g. the 8-node isoparametric brick) but the use of higher - order elements does provide a solution, albeit an expensive one.

Further development of the code will include provision for more accurate field calculations in specified volumes, either by allowing a mixture of high - and low-order elements, or simply by refining the solutions in these areas using high-order elements. An improved restart option has been added to the computer program and this has improved the efficiency by up to 60% for multiple displacements

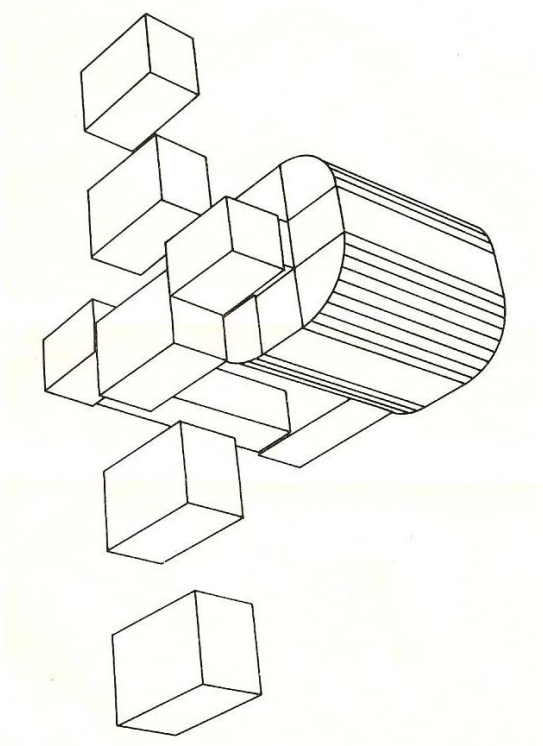

Fig. 5 *Vernier linear motor*

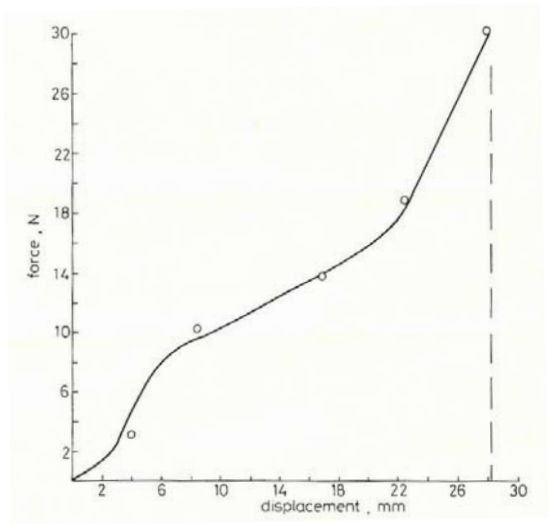

– Experimental
o Computed by TOSCA. Measurements not available beyond 28.2 mm

Fig. 6 *Computed and measured forces as a function of displacement for the vernier linear motor*

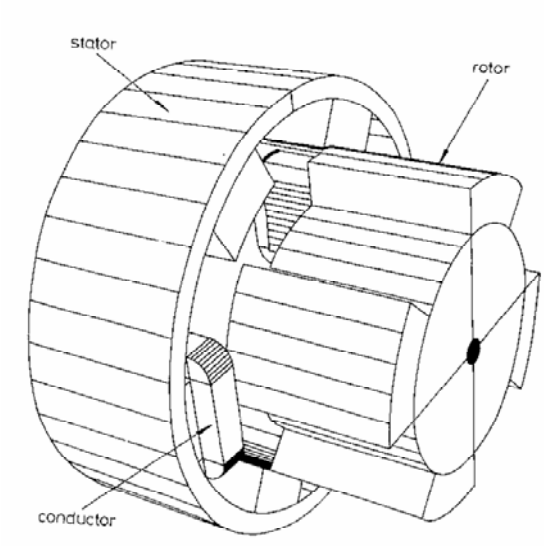

Fig. 7 *Geometry of stepping motor (rotor displaced)*

or current calculations. The main problem with the present code is preparing data. Some form of interactive pre-processor will be provided to ease this difficulty, but this must always remain a problem area. The meshing of free space makes electromagnetics rather special when compared with other problems solved by the finite-element method. Some improvement in efficiency may be obtained by using infinite elements to extend the far field boundary.

6 Acknowledgments

The authors 'are especially indebted to Dr. John Finch, formerly of UCNW, Bangor, and now at the University of Newcastle, for the experimental results from the vernier linear motor, and also to Dr. M. Stephenson and Dr. N. Fulton of the University of Leeds for experimental results in the stepping motor. They would like to thank Mrs P. Morgan for help in preparing the manuscript.

7 References

[1] ARMSTRONG, A.G.A.M., COLLIE, C.J., DISERENS, N.J., NEWMAN, M.J., SIMKIN, J., and TROWBRIDGE, C.W.: 'New developments in the magnet design program GFUN'. Rutherford Laboratory, RL-75-066, 1975

[2] TROWBRIDGE, C.W.: 'Applications of integral equation methods for the numerical solution of magnetostatic and eddy current problems'. Proceedings of International Conference on numerical methods in electrical and magnetic field problems, Santa Margherita, Italy, 1976. (Also RL-76{)71, 1976)

[3] WOLFF, W., and MULLER, W.: 'General numerical solution of the magnetostatic equations', *Wiss, Ber. AEG.Te1efuliken* 1976,49,(3),pp.77-86

[4] WINSLOW, A.M.: 'Numerical solution of the quasi-linear Poisson equation in a non-uniform triangular mesh', *J. Comput. Phys.,* 1967,2, pp. 149-172

[5] CHARI, M.W.K., and SILVESTER, P.: 'Finite element analysis of magnetically saturated de machines', *IEEE Trails., 1971,* PAS-90, pp. 2362-2372

[6] SIMIKIN, J., and TROWBRIDGE, C.W.: 'Magnetostatic fields computed using an integral equation derived from Green's theorems'. Rutherford Laboratory, RL-76-041,1976

[7] ZIENKIEWICZ, O.C., LYNESS, J., and OWEN, D.J.R.: 'Three dimensional magnetic field determination using a scalar potential', IEEE *Trans.,* 1977, MAG-13, pp. 1649-1656

[8] SIMKIN, J., and TROWBRIDGE, C.W.: 'On the use of the total scalar potential in the numerical solution of field problems in electromagnetics', *Int. J. Numer. Methods. Eng.,* 1979, 14, pp.423-440

[9] ARMSTRONG, A.G.A.M., COLLIE, CJ., SIMKIN, J., and TROWBRIDGE, C.W.: 'The solution of 3D magnetostatic problems using scalar potentials'. Proceedings of COMPUMAG conference, Grenoble, 1978. (Also RL-78-080, 1978)

[10] SMYTHE, W.R.: 'Static and dynamic electricity' (McGraw-Hill, 1968, 3rd edn.)

[11] COLLIE, C.J.: 'Magnetic fields and potential of linearly varying current or magnetisation in a plane bounded region'. Proceedings of COMPUMAG conference, Oxford,1976

[12] ZIENKIEWICZ, O.C.: 'The finite element method in engineering science', (McGraw-Hill, 1978, 3rd edn.)

[13] ARMSTRONG, A.G.A.M., COLLIE, C.J.. DIFERENS. N.J.,NEWMAN, M.J., SIMKIN, J., and TROWBRIDGE, C.W., 'GFUN3D user guide', RL-76{)29 (Rutherford Laboratory, 2nd edn., 1979)

[14] 14 MEIJERINK, J.A., and VAN DER VORST, H.A.: 'An iterative solution method for linear systems of which the coefficient matrix is a symmetric M-matrix, *Math. Comput..* January 1977 IS

[15] CARPENTER, C.J., and LOCKE, D.H.: 'Numerical models of three dimensional end winding arrays'. Proceedings of COMPUMAG conference, Oxford, 1976